RSC Advances

ROYAL SOCIETY OF CHEMISTRY

www.rsc.org/advances

RSC Advances

ARTICLE

Combined Effect of Ether and Siloxane Substituents on Imidazolium Ionic Liquids†

Received 00th January 20xx,
Accepted 00th January 20xx

DOI: 10.1039/x0xx00000x

www.rsc.org/

Santosh N. Chavan,[a] and Debaprasad Mandal*[a]

Ionic liquids (ILs) in combination with ether and siloxane substituents at the imidazolium cation comprising of bis(trifluoromethylsulfonyl)imide (NTf_2) anion have been synthesized for the purpose of low viscosity, high thermal stability and low melting or glass transition (T_g). The structural flexibility of ether and siloxane substituents on imidazolium center overcomes the effect of van der Waals force and exhibit desirable and unique physical properties. These novel ILs show low viscosity (~72 mPa.s at 25 °C), high thermal stability upto 430 °C, and wide liquid range over 500 °C. In addition, these ILs exhibit only amorphous glassy state on cooling at T_g below –74 °C and cannot order properly to afford crystallization. The detailed thermal stability, phase transitions and heat capacity were studied by TGA, DSC and temperature-modulated DSC analysis. More importantly, we have also reported the large scale (one kilogram) microwave assisted synthesis of ILs [BMIM]Br and [1O2O2Im2O1]I as an efficient and greener processes.

Introduction

Ionic liquids (ILs) were introduced initially as media for organic transformations. However, in recent years their chemistry have been developed remarkably due to their potential applications like new media for material synthesis, biocatalysts,[1] nanotechnology,[2],[3] separation techniques,[4],[5],[6] handling radioactive wastes,[7],[8] lubricant additives,[9],[10],[11] electrolytes in electrochemical devices[12],[13] and many others.[14] These ILs offers endless opportunities due to their unique properties like negligible vapour pressure (non-volatility), non-flammability, high thermal stability and wide liquid temperature range in combination with high ionic conductivity, wide electrochemical stability window and their ability to dissolve a wide variety of compounds.[1] Combination of these properties empower ILs as "greener" solvents for energy applications and industrial processes.[15],[16]

The unique properties of each IL is essentially governed by the nature of both cationic and anionic constituents and their interionic interactions. While much work has been devoted to the applications of ILs, the basic understanding and study of their structure–property relationship will be of immense benefit to fine tune the ILs with specific type of "designer medium".[17],[18] In addition, the high viscosity (η) of ILs is the major barrier for their use in most of applications. For example, in electrochemical reactions and devices, where charge carrying species essentially diffuse through the supporting electrolyte or during filtration, pumping, dissolution, separation and mixing.

During the last few decades numerous studies have been devoted in reducing the viscosity and melting points of ILs by altering the anion employed. For example, bis(trifluoromethylsulfonyl)imide [Tf_2N; TFSI], and dicyanamide [$(CN)_2N$] are the optimum choice of anions to keep the viscosity low.[19] However, recently the functionality of cations also attracted a great attention for regulating the viscosity. Attachments of hetero atom containing substituents, like alkoxy (R-O-R) and siloxy (Si-O-Si) groups with imidazolium, phosphonium or ammonium cations are shown to be effective in decreasing the viscosity dramatically due to increase in free rotation around the hetero atom.[20],[21],[22],[23],[24] Further, the alkoxy chain effect on decreasing the viscosity was ascribed to the high conformational flexibility of the ether moieties and provides more available holes for the convenience of mass transport and low viscosity.[21, 25] For example, alkoxy functionalized quaternary ammonium ILs offer enough flexibility to reduce the viscosity relative to the isoelectronic alkyl chains and they have been used as high-conductive electrolytes.[22a] However, thermal stability would be a major concern due to favourable elimination reaction facilitated by electron withdrawing nature of alkoxy groups. Whereas, the attachment of siloxy group not only gives conformational flexibility similar to alkoxy but also improves the thermal stability. However, addition of siloxane or ether fragments to ILs wouldn't alter their toxicity significantly. Also, due to highly hydrophobic nature of siloxanes, the solubility of the ILs in different solvents is expected to be altered.

Given, the individual study on alkoxy and siloxy substitutents to ILs, the studies on the combination of these two in ILs are still not been reported. Hence, we consider the

[a] Department of Chemistry, Indian Institute of Technology Ropar, Punjab 140001, (India), E-mail: dmandal@iitrpr.ac.in

† Dedicated in memory of Prof. B. D. Gupta, IIT Kanpur.

Electronic Supplementary Information (ESI) available: Details for synthesis, characterization, TGA, DSC and TOPEM graphs See DOI: 10.1039/x0xx00000x

combined effect of these two functional moieties alkoxy and siloxy in an ionic liquid to ascertain all-in-one aforementioned essential features like low viscosity, good thermal stability and a wide liquid range. In the present study, we have designed four novel ILs combining both alkoxy and siloxy substituents on imidazolium cation with TFSI anion as shown in Figure 1 and reported the detailed studies on viscosity, thermal stability, phase transitions and heat capacity.

ILs **1** and **2** are 1-alkoxy-3-siloxy imidazolium salts. The less toxic silyl or siloxane polymers are extensively used in medical applications (implants) and in personal care products like, in baby bottle teats. ILs **3** and **4** are designed for the comparison of physical properties and better understanding the structure-property relationships. The physical properties of ILs **1-4** were validated with respect to BMIM TFSI (**5**), which is considered as the most studied IL reported in the literature.

More importantly, we have also explored an efficient microwave (MW) assisted method for producing large quantities of high quality ionic liquids in kilogram scale. To the best of our knowledge, the large scale synthesis of ILs over a kilogram scale was only reported using conventional heating method by Burrell et. al.[26] Microwave assisted synthesis has importance as a valuable, greener and efficient alternative for functionalized IL.[27]

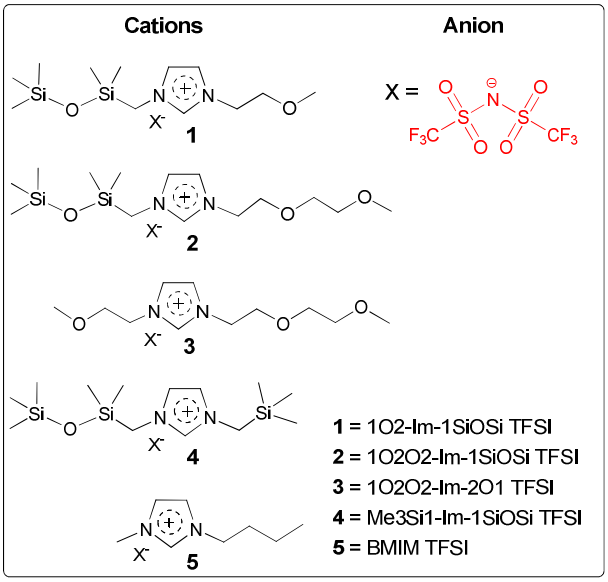

Figure 1. Ionic liquids used in this study.

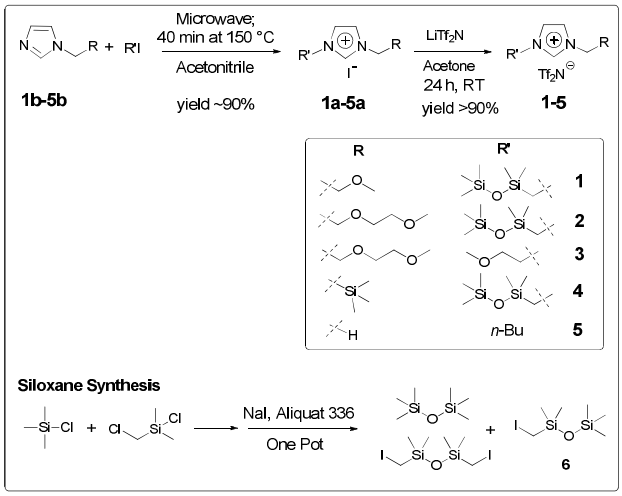

Scheme 1. Synthesis of ionic liquids **1**-**5**.

Results and discussion

Synthesis

Five unsymmetrically substituted imidazolium ionic liquids (**1-5**, Figure 1) with Tf_2N anion were synthesized from corresponding imidazolium iodides (**1a-5a)** with more than 90% yield and >99% purity. The purity of all ILs were analyzed primarily by ^1H, ^{19}F NMR and mass spectroscopic techniques. ILs **1**, **2**, **4** are highly hydrophobic, therefore washing with deionized water offer high purity ILs and the halide removals was confirmed by $AgNO_3$ test. However, IL **3** is less hydrophobic compared to other ILs due to the presence of ether functionality on the both sides of imidazolium ring and the yield tend to reduce during washing with deionized water.

Corresponding imidazolium iodides (**1a**-**5a**) were synthesized from respective N-substituted imidazole (**1b**-**5b**) by microwave irradiation in a batch scale of ~50 mmol in the presence of acetonitrile as solvent (solvent was added to fill the minimum volume of microwave oven vials ~6 mL) for 40 min (Scheme 1). Large scale microwave synthesis 2000 mmol of [1O2O2-Im-2O1]I (**3a**) and [BMIM]Br (**5a**) were also tested in a batch of 8 Teflon vials rotor of 100 mL capacity in solvent free condition to assess the scope of greener/scale-up methods and ILs were synthesized at almost half a kilogram scale with 99% yield and 77% of the excess halide used in reaction was recovered by simple decantation and distillation. It is also possible to scale-up the MW synthesis with 16 vial rotor for more than a kilogram scale.

ILs **1** and **2** were prepared from the reaction of ether substituted imidazole (**1b** and **2b**) and iodomethyldimethyldisiloxane (**6**). The disiloxane precursor **6** was prepared from chloromethyldimethylchlorosilane (**7**) by iodination in presence of phase transfer catalyst, Aliquat 336®. Phase transfer catalyst reduces the halide exchange reaction time and also increases the yield. The chloromethyl silane compound **7** when used for quaternization (**1a** and **2a**) the

obtained yield was poor along with impurities, whereas the iodide precursor gives clean reaction with better yield (~90%).

Table 1. Density of ILs **1-5** at 25 °C.

ILs	Density (g/cm^3 at 25 °C)	Mol. wt
1O2-Im-1SiOSi TFSI (**1**)	1.3036	567.67
1O2O2-Im-1SiOSi TFSI (**2**)	1.2935	611.72
1O2O2-Im-2O1 TFSI (**3**)	1.4155	509.07
Me3Si1-Im-1SiOSi TFSI (**4**)	1.2520	595.80
BMIM TFSI (**5**)[a]	1.4365	419.36

[a] (at 25 °C BMIM TFSI 1.436 g/cm^3)[18b].

Solubility/miscibility. The ILs **1**-**5** are highly miscible in chloroform, dichloromethane, THF, acetone and benzene but immiscible in water and hexane and slightly miscible in ether. ILs **1**-**5** are also freely miscible in propylene carbonate which is a good solvent to aid electrochemical analysis.

Characterization

NMR. C2 proton (H_{C2}) of imidazolium ring is a good measure to ascertain reaction progress and purity. While H_{C2} appeared at ~10 ppm with the halide anion but exhibits upfield shift to ~8 ppm with TFSI. This is also a good indication of the interaction between cation and anion which mainly reflects the unique properties of ILs. Tf_2N (CF_3) appears at –78 ppm in ^{19}F NMR for ILs **1**-**5** and there is almost no shift observed for different Ils.

Density. The density of ILs **1-5** were measured with small variation of temperature and the density values at 25 °C are given in Table 1 and more details are provided in Figure S1 [supporting information (SI)].

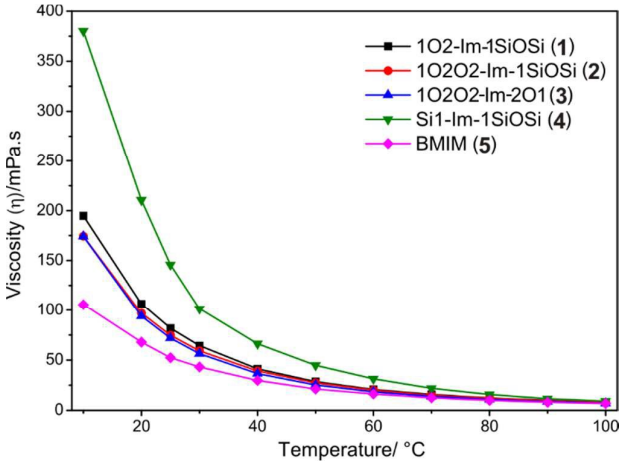

Figure 2. Plot of dynamic viscosity (η, estimated error ±3%) *vs*. temperature for ILs **1**-**5**.

Table 2. The dynamic viscosity (η /mPa·s) with change in temperature of ILs **1-5.**

Temp. (°C)	1O2-Im-1SiOSi (**1**)	1O2O2-Im-1SiOSi (**2**)	1O2O2-Im-2O1 (**3**)	Me3Si1-Im-1SiOSi (**4**)	BMIM (**5**)
10	194.7	174.2	174.1	380.2	105.7
20	106.5	96.97	94.0	202.4	68.0
25	81.9	74.7	71.9	144.9	52.3
30	64.3	59.2	56.3	111.4	43.2
40	41.3	39.2	36.4	66.3	29.7
50	28.6	27.3	25.1	44.9	21.2
60	20.8	20.0	18.3	31.4	16.4
70	15.7	15.2	13.8	21.9	12.4
80	12.2	11.9	10.8	15.7	9.8
90	9.8	9.5	8.7	11.5	8.0
100	7.9	7.6	7.1	9.3	6.7

Viscosity. ILs with low viscosity are desirable to facilitate the mass transport when applied as media in most of their applications. The viscosity of an ionic liquid is significantly governed by the molecular symmetry, ion sizes and the interionic interactions (such as van der Waals force and electrostatic attractions).[28] The viscosities for ILs 1O2-Im-1SiOSi TFSI (**1**), 1O2O2-Im-1SiOSi TFSI (**2**), 1O2O2-Im-2O1 TFSI (**3**), Me3Si1-Im-1SiOSi TFSI (**4**) and BMIM TFSI (**5**) with varying temperature in an inert atmosphere are listed in Table 2 and a plot of viscosity *vs*. temperature is shown in Figure 2. All five ILs follow the Vogel–Tammann–Fulcher (VTF) equation[29] for viscosity with variation in temperature.

$$\eta = \eta_0 \exp[B/(T-T_0)]$$

Where η is viscosity, T is the absolute temperature, η_0 (mPa.s), B (K), and T_0 (K) are adjustable parameters for VTF equation. η_0 is the pre-exponential parameter, (a reference viscosity at which the exponential term approaches unity i.e., high temperature asymptote), B is called pseudoactivation energy, and T_0 is coincide to ideal glass transition temperature.

Table 3. VTF equation parameters of viscosity for the ILs.

ILs	η_0 (mPa.s)	B (K)	T_0 (K)	R^2
1O2-Im-1SiOSi TFSI (**1**)	0.192±0.01	725±12.7	184.4±0.23	0.9999
1O2O2-Im-1SiOSi TFSI (**2**)	0.233±0.01	679.2±11.9	180.3±1.02	0.9999
1O2O2-Im-2O1 TFSI (**3**)	0.216±0.01	659.5±2.6	184.4±0.23	0.9999
Me3Si1-Im-1SiOSi TFSI (**4**)	0.039±0.02	1196.5±185	152.6±11.1	0.9996
BMIM TFSI (**5**)	0.070±0.04	1057±189	138.0±14.5	0.9992

The best-fit parameters η_0 (mPa.s), B (K), and T_0 (K) are given in Table 3 along with corresponding fitting coefficient R^2 values. From tabular data of VTF equation it is clear that if T_0 values are smaller, then B is bigger and the viscosity would be more sensitive to temperature. ILs **1-3** has similar η_0 and T_0 values, but IL **1** gives higher B values among ILs **1-3**. However, the B and T_0 values do not show a regular relation with the structures of cations

BMIM TFSI (**5**) shows η as 52.3 mPa.s at 25 °C which are in good agreement (51.7 mPa.s) with the reported literature.[25] Viscosity of ILs **1**, **2** and **3** are 81.9, 74.7 and 71.9 mPa.s at 25 °C respectively, which are reasonably less viscous in spite of their high molar mass. Although, the viscosities of ILs **1-3** are little higher than BMIM TFSI (**5**), but one should not compare the viscosity of these double functionalized ILs (**1-3**) with low mol. wt. alkyl substituted BMIM.

Further, IL **3** (Mw = 505.5) shows the lowest viscosity but interestingly does not increase much for ILs **1** and **2** with considerable increase in molecular weight (Mw) upon attachment of Si-O-Si group [Mw = 567.7 (IL **1**), 611.7 (IL **2**)]. Since the electronic and geometric structure of the imidazolium ring remains unaffected by the functionalization of the alkyl chains, the primary interaction between the imidazolium ring and TFSI anion will be quite similar among these ILs **1-5**. Due to minimum basicity and good charge delocalization of TFSI, van der Waals forces is expected to be dominating over interionic electrostatic interaction between imidazolium cation and TFSI. Again the van der Waals forces mostly depend on the molar mass and the side chains. Sufficient side chain mobility of ether and siloxane moieties in ILs **1-3** out-weighs the increase in the molar mass. This is also reflected in ^{1}H NMR δ^1H_{C2} (imidazole) which correlates well with the cation/anion interaction. For example, δ^1H_{C2} (imidazole) shifted downfield by ~2 ppm in ILs **1-5** with TFSI compared to halides (**1a-5a**). However, δ^1H_{C2} (imidazole) doesn't show any noticeable shift within ILs **1**-**5** indicating similar interionic interactions. This signifies the effect of side chain functionality on viscosities.

Compare to IL **1**, with increasing the alkoxy chain length in IL **2**, the η value decreases by 10 mPa.s at 20 °C, which is opposite to the trend from the literature reported ILs [Me-Im-2O1]TFSI[25] *vs.* [Me-Im-2O2O1]TFSI[30]. It seems there is considerable effect of Si-O-Si (siloxane) functionality on the viscosity of IL **1** and **2**. Again, IL **2** shows similar viscosity with [Me-Im-1SiOSi]TFSI (η = 75.6 mPa.s at 25 °C)[31]. Whereas, the η value increases almost 20 mPa.s in IL **3** compare to [Me-Im-2O2O1]TFSI (η =70.3 mPa.s at 21 °C). These comparisons point towards the fact that the viscosity remains similar in spite of the increase in the molar mass in ILs **1-3**.

Surprisingly the IL **4**, which is a combination of Me3Si1 and Si-O-Si1 shows higher viscosity (η =144.9 at 25 °C) than ILs **1-3**. In comparison to IL **4**, the η values of Me-Im-1Si-O-Si TFSI and Me-Im-1SiMe3 at 25 °C are 89.0 and 97.7 respectively. The effect of CH_2SiMe_3 is not similar here to keep the viscosity low. The molar volume (Mol. wt./density) of IL **4** is highest among ILs **1-5** due to lower density. Possibly, the trend that low viscosity stems from high molar volume does not keep up here.

The viscosity in these imidazolium ILs seems to be governed by two major factors 1) interionic interactions and 2) side chain mobility. Since the primary interaction between the TFSI anion with imidazolium core structure essentially remain same, we consider the electronic and structural effect of the sidechains that are related to van der Waals forces. Hence, the contribution of each alkoxy and siloxy chains are important. The alkoxy groups in IL **1-3** were carefully chosen with two CH_2 spacers (Im-2O1 or Im-2O2O1) at the imidazolium attachment to reduce the electron withdrawing effect of alkoxy group. The sidechain flexibility of alkoxy group effectively influence the viscosity. The siloxanes (Si-O-Si), not only imparts the sidechain mobility but, the electron donating effect of CH_2-Si-O-Si also decreases the partial positive charge and consequently the interionic interaction.

The Newtonian behavior of these ionic liquids (**1-5** and **1a-5a**) were also tested on Rheometer at 25 °C in ambient atmosphere by varying shear rate and represented in Figure S2 (SI). ILs **1**-**3** and **5** with TFSI anion exhibit Newtonian behavior as the viscosity remains constant with varying shear rate. But ILs with halide anion (**1a**-**3a**) shows gel type shear thinning behavior as shown in Figure S3 (SI). The viscosity determined by Rheometer shows lower values than measured by viscometer due to the influence of moisture while carrying out the measurement by Rheometer in open-air atmosphere.

Thermal Characterization

Thermal stability. The thermal stability of these ILs were determined by thermogravimetric analysis and the TGA curves are shown in Figure 3. The thermal decomposition temperature (T_d) is considered as the onset temperature in TGA curve. The dynamic TGA results as shown in Table 4 exhibits excellent short term stability over 400 °C at a scan rate of 10 °C/min. The onset temperature of mass loss for ILs **1**, **2**, **3** and **4** show the T_d as 430.4, 430.4, 426.8 and 413.6 respectively, which are quite similar due to the basic imidazolium structure of all four ionic liquids with TFSI as anion. [BMIM]TFSI (**5**) shows higher decomposition temperature at 440.4 °C compare to other ILs. The observed thermal decomposition of [BMIM]TFSI is well within the limits as reported in the literature (T_{onset} = 442[32] or 439 °C[33]).

ILs **1**, **2**, and **3** have comparable T_d, as was observed in the case of viscosity. Very high T_d of ILs **1** and **2** indicate that the electron withdrawing effect of alkoxy on imidazolium core is cancelled out by the electron donating and hyperconjugation effect of disiloxane, which causes improved thermal stability. IL **4** surprisingly shows slightly lower thermal decomposition temperature T_d.

Pyrolysis of the imidazolium salts with different halide anions is known to proceed most likely via S_N2 process depending on the basicity and/or nucleophilicity of the anions.[34] However, in presence of TFSI anion the pyrolysis proceeds via S_N1 reaction and the thermal stability is governed

by the difference in inductive effects of the side chain attached to N-atom.

Based on the DTG curves (first derivative of TGA, Figure 3) a stepwise decomposition was observed for all the ILs except **5** (BMIM TFSI). IL **3** exhibits overlapping of two continuous degradation steps. Whereas, ILs **1** and **2** clearly shows three degradation steps which can be assigned to characteristic decomposition reaction. Assuming S_N1 type degradation, the first step showing a small hump with 10% weight (wt.) loss in IL **2** is possibly due to evaporation of ether substituent. Next two big humps corresponds to $[Im\text{-}Si\text{-}O\text{-}Si]^+$ (accounts for 40% wt. loss) and in the end TFSI (accounts for 50% wt. loss). IL **2** shows exactly similar degradation pattern with a small hump (17% wt. loss) as first step. This was followed by two large humps of 37% and 46% wt. loss corresponding to $[Im\text{-}Si\text{-}O\text{-}Si]^+$ and TFSI respectively. Although, the thermogravimetric analysis does not provide a mechanism of the evaporation process, the weight loss indicates that the decomposition initiates at the ether attachment at least in **1** and **2** under the prevailing conditions. Simultaneously, IL **4** shows two steps of decomposition which closely matches with the corresponding % wt. loss of the components, Me_3SiCH_2 (15%), [Im-Si-O-Si] and TFSI (85%). All samples preferably show dominant mass-loss at T_{endset} (above 490 °C) with left over residue of 3-5%, except for IL **3** where the residue was 8%.

Table 4. Dynamic TGA data of ILs **1-5**.

ILs	T_{start} (°C)	T_{onset} (°C)	T_{peak} (°C)	T_{endset} (°C)
1O2-Im-1SiOSi (**1**)	288.1	430.4	473.6	493.3
1O2O2-Im-1SiOSi (**2**)	307.4	430.4	483.0	498.1
1O2O2-Im-2O1 (**3**)	309.7	426.8	480.5	494.7
Si1-Im-1SiOSi (**4**)	309.3	413.6	471.2	486.4
BMIM (**5**)[a]	326.1	440.4	489.6	503.9

[a] Literature reported BMIM TFSI data T_{start} (330 °C[32]) and T_{onset} (442 °C[32], 439 °C[33])

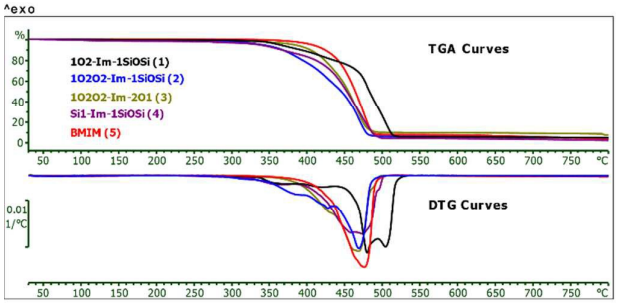

Figure 3. Dynamic TGA and DTG curves of ILs **1-5**.

Table 5. Isothermal TGA of ILs **1-5**.

ILs	Temperature (°C)	% wt Loss in 4 h
1O2-Im-1SiOSi (**1**)	250	13.5
1O2O2-Im-1SiOSi (**2**)	280	16.3
1O2O2-Im-2O1 (**3**)	280	8.7
Si1-Im-1SiOSi (**4**)	280	13.9
BMIM (**5**)	310	10.6

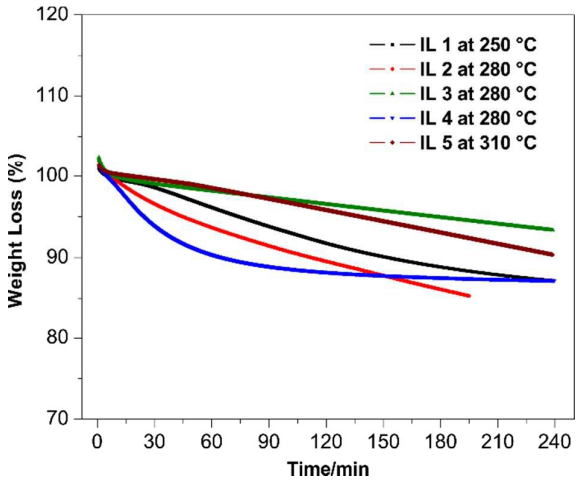

Figure 4. Isothermal TGA curves of ILs **1-5**.

The long term thermal stability was also investigated by performing isothermal TGA in N_2 atmosphere for 4 h at a given temperature. The temperature chosen was ~30 °C below the T_{start}. The long-term stability of these ILs are important from industrial application point of view.[35] The data and nature of isothermal TGA curve are depicted in Table 5 and Figure 4 respectively. From the slope of isothermal TGA curves, it can be predicted that IL **3** has the best long term stability among the studied ILs, even better than IL **5** (BMIM TFSI). Comparing T_{onset}, ILs **1** and **2** (ether/siloxane) are more stable than **3** (ether-ether); also, T_{start} for **2** and **3** are comparable in TGA. However, it is found that IL **1** and **2** exhibits lower long term thermal stability than **3**. It can be predicted from DTG curve, where the ether group evaporated first in S_N1 type degradation leaving $[Im\text{-}Si\text{-}O\text{-}Si]^+$. $[Im\text{-}Si\text{-}O\text{-}Si]^+$ gain extra stability due to the +I effect of [Si-O-Si] group and facilitate the degradation than in IL **3** (Ether-Im-Ether) where the $[Im\text{-}Ether]^+$ part is unstable due to –I effect of ether group.

Phase transitions and Heat Capacity (C_p) in DSC and Temperature-Modulated DSC. The phase transitions like the glass transition (T_g), cold crystallization (T_c), and melting temperature (T_m) were observed during DSC measurement from -90 to 20 °C and were further confirmed by performing TOPEM® a temperature-modulated DSC analysis program. The

DSC measurement was performed from –90 to 20 °C and TOPEM was carried out from –90 to 60 °C.

The heating scans show only glass transitions (T_g) in DSC as well as in temperature-modulated DSC scan for ionic liquids **1**, **2**, **3**, and **4** and the respective T_g values are –74.4, –72.3, –74.6 and –63.2 °C respectively. The glass transitions (T_g) and corresponding enthalpies relaxation (ΔH_g) of ILs **1-5** are given in Table 6 and the DSC curves are shown in Figure 5, and Figure S4 (SI). The enthalpy relaxation ΔH_g of 1O2O2-Im-SiOSi TFSI (**2**) is 8.56 KJ/mol, which is highest among these ILs. The siloxane substituted ILs give higher ΔH_g than ether or alkyl substituents. BMIM TFSI (**5**) shows only T_g at –88.3 °C and we do not observe the cold crystallization and melting during DSC measurement. However, temperature-modulated DSC (TOPEM) analysis clearly shows the cold crystallization (T_c), and melting temperature (T_m) to be –40.9 and –5.0 °C respectively. According to literature the T_g, T_c, and T_m for BMIM TFSI are –87, –40 and –7 °C respectively.[18b, 32]

Table 6. DSC data of ILs **1-5** with the enthalpy relaxation at glass transition (ΔH_g).

ILs	T_g (°C)	ΔH_g (KJ/mol)
1O2-Im-1SiOSi (**1**)	–74.4	1.873311
1O2O2-Im-1SiOSi (**2**)	–72.3	8.56408
1O2O2-Im-2O1 (**3**)	–74.6	1.374489
Si1-Im-1SiOSi (**4**)	–63.2	5.24304
BMIM (**5**)[a]	–88.3	1.216144

[a] BMIM TFSI T_g (–86 °C[32], –87 °C[18b]), T_c (–44 °C[32]), T_m (–2 °C[32], –6 °C[18b]).

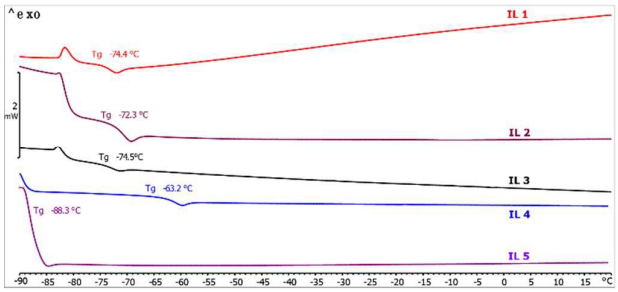

Figure 5. The heating DSC thermograph of five ionic liquids. Upward peaks are considered as exothermic

The DSC curves for ILs **1**, **2** and **3** show artefact peaks at initial position in low temperature region, which was not observed in TOPEM. One peculiar observation is that IL **4** gets solidified under open atmospheric conditions and at ambient temperature possibly due to absorption of moisture from atmosphere. However, when DSC analysis was performed with solid IL **4**, only the first scan shows the sample melted in the temperature range 26-28 °C but subsequent cooling or heating cycles lack any further instances of solidification or melting. Even during the TOPEM measurement melting was not observed for IL **4**.

Table 7. Heat capacity (C_p) values of ILs (**1-5**) in temperature-modulated DSC (TOPEM) at T_g, 25 and 50 °C.

	T_g		25 °C		50 °C	
ILs	C_p (J/g·K)	C_p (J/mol·K)	C_p[a] (J/g·K)	C_p[b] (J/mol·K)	C_p (J/g·K)	C_p (J/mol·K)
1O2-Im-1SiOSi (**1**)	1.09	618.7	1.23	698.2	1.25	709.6
1O2O2-Im-1SiOSi (**2**)	1.18	721.8	1.41	862.5	1.39	850.3
1O2O2-Im-2O1 (**3**)	1.14	580.3	1.38	702.5	1.40	712.7
Si1-Im-1SiOSi (**4**)	1.03	613.7	1.19	709.0	1.20	715.0
BMIM (**5**)	1.14	478.1	1.30	545.2	1.32	553.5

[a] specific heat capacity; [b] molar heat capacity

Many ionic liquids tend to crystallize pretty slowly, however, it is still possible to detect these phase transitions in TOPEM by employing slow heating rates. DSC scans with heating and cooling cycle for all four ILs show no signs of freezing or melting transitions, even during TOPEM. It is evident that the ILs remained in the liquid state for the entire dynamic ranges of study reported here. Therefore ILs **1**, **2** and **3** depict the formation of only glassy state due to high mobility of side chains, which could not orient properly even at 2 °C/min heating rate during TOPEM measurement. Owing to lack of melting, the liquid range of these ILs (**1-3**), may be considered as the difference between glass transition temperature (T_g) and thermal decomposition temperature (T_d), which is over 500 °C.

Heat capacity (C_p): The heat capacity (C_p) of ILs **1-5** were determined from TOPEM scan ranging from –90 °C to 60 °C at a heating rate of 2 °C/min. The respective C_p values at T_g, 25 and 50 °C are given in Table 7 and the detail of TOPEM graphs are shown in Figure S5 (SI). Since specific heat capacity is an important parameter that ought to be considered for ILs since they are good candidates as thermal fluids.[36] IL **2** exhibits the highest heat capacity among all the ILs in present study considering either the molar or specific heat capacity. IL **4** has lowest heat capacity (C_p) due to the presence of Si containing groups on both side of imidazolium ring. Heat capacity of ILs **1-5** tend to increase with increase in temperature which is obvious and follow the general trend. For example, molar heat capacity increased by ~10 J/mol on increasing temperature from 25 °C to 50 °C in **1-5**. However, IL **2** exhibit some heat exchange incident close to 50 °C (Figure S5, SI) and shows lower C_p during this process compare to 25 °C.

Conclusions

Efficient microwave assisted bulk scale (Kg scale) synthesis of ILs resulted in high yield along with excellent purity. The

ether/siloxane ILs exhibited large liquid range over 500 °C from –74 °C to 430 °C with a decent low viscosity (~72 mPa.s at 25 °C). The combined effect of ether and siloxane substituent in imidazolium cation overcomes the columbic packing force, van der Waals force, size factor and conformational degree of freedom. Development of ILs while considering structure-activity relationship seems to be effective approach. In recent work, we found that similar effect of substituents are also effective on different ammonium and phosphonium cations for controlling the desirable features of ILs and these systems will be described in subsequent reports.

Experimental

General. Glassware were oven-dried prior to use and all reactions were conducted in an inert atmosphere unless otherwise specified. Aqueous solutions were prepared with deionized water (Millipore). All ILs were vacuum dried at 60 °C and 10^{-3} mbar for 6-10 h before performing each test. The microwave assisted reactions were carried out in Muiltiwave Pro instrument from Anton Paar. In this system two standard magnetrons of 850 W deliver up to 1500 W microwave power in an unpulsed mode over the full power range.

Materials. Chemicals like hexane, chloroform, diethyl ether, ethyl acetate were purified by simple distillation. Tetrahydrofuran was passed through neutral alumina followed by distillation over Na/benzophenone. Acetone was freshly dried over KOH and CaH_2 respectively followed by distillation. Acetonitrile and dichloromethane distilled over P_2O_5. Imidazole (Alfa, 99.5%); 2-Methoxymethanol (Spectrochem, India, 99.5%); 2-(2-Methoxy-ethoxy)-ethanol (SD Fine, India, 98.0%); *p*-Toluene sulphonyl chloride (SD Fine, India, 99.0%); Chlorotrimethylsilane (TCI, 98%); Chloro(chloromethyl)dimethylsilane (Sigma Aldrich, 98%); NaI (Alfa, 99%); Bis(trifluoromethanesulfonyl)imide lithium salt (TCI, 98%); and Chloroform-d (Sigma Aldrich, 99.8 atom % D) were used as received.

Characterization methods

NMR spectroscopy. NMR spectra were recorded using a JEOL JNM-ECS 400 spectrometer at ambient probe temperatures and referenced as follows: ^{1}H: residual internal $CHCl_3$ (δ = 7.26 ppm); ^{13}C internal $CDCl_3$ (δ = 77.16 ppm); **FT-IR.** FT-IR spectra were recorded as neat with ATR on BRUKER TENSOR-27 spectrometer in the range of 600-4000 cm^{-1} (Spectral Resolution = 4 cm^{-1}; Number of scans = 100). **GC-MS Spectrometry.** The mass spectra was recorded by GC-MS (QP2010 Ultra, Shimadzu Corporation). The direct probe EI-MS mode was used for data collection with 50 eV ion electron energy.

Density Measurement. The density measurements were performed between 20 °C and 40 °C in an inert atmosphere using DMA 35 portable density meter from Anton Paar, which was calibrated using ultrapure water (0.99704 g/mL at 25 °C). The IL samples were previously degassed under vacuum at 60 °C overnight and loaded without any atmospheric interference. Each test was repeated at least thrice.

Measurement of water content. The water content in ILs **1**-**5** were determined after vacuum drying at 60 °C and 10^{-3} mbar for 8 h by Karl Fisher titration using a C20 Karl Fisher Coulometer (Mettler Toledo), with diaphragmless cell and dual platinum electrode sensor. For an analytical process HYDRANAL® Coulomat AG anolyte water standards from Fluka® analytical was used. The moisture content of these ILs **1**-**5** was determined by Karl-Fisher titration in the range 200 to 400 ppm.

Viscosity. Viscosity was measured in an inert atmosphere on Lovis 2000M Microviscometer from Anton Paar with temperature scan ranging from 10 °C to 100 °C at a heating rate of 5 °C/min. Each measurement was repeated at least thrice and presented data is averaged out with an error limit of 3% (standard deviation less than 2 mPa.s). Stainless steel balls having diameter of 1.5 mm, density 7.7 g/cm^3 and running path of 20 cm were used in three different capillaries of diameter 2.5 mm, 1.8 mm, and 1.59 mm respectively, with the respective viscosity range being 700–1500 mPa.s, 30–700 mPa.s, and 2.5–60 mPa.s. The Newtonian test and viscosity measurements were carried out under atmospheric condition on an Anton Paar Rheometer Model: MCR102 SN81403820; FW3.80; Slot (3,-1); Adj (9,0)d, Measuring System: PP25-SN34217; [d=0.1 mm], Peltier temperature control. The temperature range of analysis was from –5 °C to 120 °C at the heating rate 0.2 °C/s.

Thermal Analysis. The thermal decomposition temperature was recorded in nitrogen atmosphere by thermogravimetric analysis (TGA) technique on a "TGA/DSC 1" instrument with SDTA sensor from Mettler Toledo. The thermal data were analyzed in STAR^e software. The temperature, weight and tau lag was calibrated using the Aluminum/Zinc standard sample. High purity nitrogen (99.999%) was passed at a flow rate of 40 mL/min throughout the experiments to avoid contamination from the external atmosphere. The experiments were performed using alumina pan for sample holder and as reference by using 5-20 mg samples. Thermal stability was investigated by heating from 30 °C to 800 °C at a heating rate of 10 °C/min. Each sample was tested for at least three times and the error limit is <2%. The measurement of phase-transition temperature and heat capacities were recorded by differential scanning calorimeter (DSC) using a DSC1/700W with HSS8 high sensitivity sensor instrument (Mettler Toledo) with Huber TC100MT Intercooler and Olympus microscope attachments. Data were analyzed in the STAR^e software. The temperature, heat change and tau lag was calibrated using the pure Indium/Zinc standard sample (In/Zn 156.6/419.5 °C). The DSC was also calibrated with deionized water for low temperature measurements. Standard aluminum pan with pin was used as reference. The samples were heated at 120 °C and held for 10 min isothermally to allow the evaporation of volatile impurity like moisture. The DSC measurements were performed successively through a heat-cool-heat (either 3 or 5 steps) program to ensure the phase transitions, as follows:

step 1: cooling from 25 °C to –90 °C at a rate of 5 °C/min and held for 5 min; step 2: heating from –90 °C to 20 °C at a rate of 5 °C/min and again held 5 min; step 3: cooling from 20 °C to –90 °C at a rate of 5 °C/min and held for 5 min; step 4: heating from –90 °C to 20 °C at a rate 5 °C/min. These ILs were thermally annealed by repeatedly cycling and/or holding the samples at sub-ambient temperatures for varying period of time to allow a complete crystallization. The heat capacity and heat flow were calculated from TOPEM®, a temperature-modulated DSC technique by using a heating method –90 °C to 60 °C at a rate of 2 °C/min. The temperature-modulated DSC (TOPEM®) technique allows non-reversing effect i.e. kinetic events such as reorganization, crystallization, crystal perfection, cure, decomposition and stress relaxation to be separated from reversing effect such as glass transition.

Syntheses.

In a typical synthetic procedure for preparation of ionic liquid 1O2O2-Im-2O1 TFSI (**3)** as an example. A mixture of N-alkoxy imidazole (**2b**), 1O2-I (**10**) and acetonitrile prepared in Ar/N_2 atmosphere was transferred into microwave Teflon vials. The sample was microwave irradiated by controlled temperature programming at 150 °C by 2 min ramp and held for 40 min at 150 °C, under a limiting pressure of 18 bar and 500 W power. The reaction progress was monitored by TLC, and ^{1}H NMR. After completion of reaction, concentrate the reaction mixture via *rotavac.* A viscous precipitate was obtained by drop wise addition of residue in cold ether. The biphasic system was kept at 0 °C for 2 h. Ether layer was decanted and the residue washed with cold ether (50 mL × 3). The yellow viscous liquid was subsequently dried in vacuum at 60 °C. The obtained product was then placed for anion exchange with LiTFSI at ambient temperature in acetone. After completion of reaction the product was washed with water (40 mL × 5) and the halide ion concentration was anticipated by $AgNO_3$ test. The color impurity was removed by activated charcoal. Ionic liquid **1** and **2** containing siloxane and ether substituent has been prepared similarly starting from **2b**. The detailed procedure is given under preparation method.

1-(2-methoxyethyl)-3-((1,1,3,3,3-pentamethyldisiloxanyl)methyl)-1H-imidazol-3-ium bis((trifluoromethyl)sulfonyl)amide (1): A RB flask was charged with **1a** (7.202 g, 17.38 mmol), LiTFSI (5.987 g, 20.85 mmol), and 25 mL of acetone. The reaction mixture was stirred at ambient temperature for 24 h. Acetone was then evaporated at reduced pressure. The product was washed with cold water (5 mL × 4) and dried under high vacuum at 50 °C for 4 h to afford **1** (8.973 g, 15.81 mmol, 91%). Colour impurities were removed by activated charcoal; anion exchange and iodide removal was confirmed by $AgNO_3$ test and chemical shift of δH_{C2} in ^{1}H and ^{19}F NMR.
NMR: (^{1}H, $CDCl_3$) δ ppm: 8.55 (s, 1H, NC*H*N), 7.42 (t, *J*=1.5 Hz, 1H, NC*H*CHN), 7.16 (t, *J*=1.6 Hz, 1H, NCHC*H*N), 4.33 (t, *J*=4.5 Hz, 2H, NCH_2CH_2O), 3.74 (s, 2H, NCH_2Si), 3.77 (t, *J*=4.5 Hz, 2H, NCH_2CH_2O), 3.33 (s, 1H, OCH_3), 0.18 (s, 6H, $Si(CH_3)_2$), 0.06 (s, 9H, $Si(CH_3)_3$). **(^{13}C {^{1}H}, $CDCl_3$)** δ ppm: 135.48 (s, NC*H*N), 123.18 (s, NC*H*CHN), 122.80 (s, NCHC*H*N), 119.89 (q, *J*=321.1 Hz, CF_3), 70.01 (s, NCH_2CH_2O), 58.95 (s, NCH_2Si), 49.90 (s, NCH_2CH_2O), 42.39 (s, OCH_3), 1.73 (s, $Si(CH_3)_2$), –1.18 (s, $Si(CH_3)_3$). **(^{29}Si {^{1}H}, $CDCl_3$)** δ ppm: not detected (s, $Si(CH_3)_2$), 2.86 (s, $Si(CH_3)_3$). **(^{19}F $CDCl_3$)** δ ppm: –78.91 (s, CF_3). **MS m/z (EI):** 552.25, 287.35, 271.10, 257.80, 229.35, 183.74, 141.10, 140.10, 83.10. **IR** (neat): 3150.9 w, 2959.2 w, 1562.7 w, 1350.4 m, 1184.6 s, 1053.6 s, 843.1 s.

1-(2-(2-methoxyethoxy)ethyl)-3-((1,1,3,3,3-pentamethyldisiloxanyl)methyl)-1H-imidazol-3-ium bis((trifluoromethyl)sulfonyl)amide (2): The reaction/workup given for **1** was repeated with **2a** (8.129 g, 17.73 mmol), LiTFSI (6.108 g, 21.28 mmol), and 25 mL of acetone. This gave **2** as light yellow oil (9.767 g, 15.97 mmol, 90%).
NMR: (^{1}H, $CDCl_3$) δ ppm: 8.71 (s, 1H, NC*H*N), 7.47 (t, 1H, *J*=1.8 Hz, NC*H*C), 7.13 (t, 1H, *J*=1.8 Hz, NC*H*C), 4.36 (t, 2H, *J*=4.54 Hz, NCH_2CH_2), 3.78 (t, 2H, *J*=4.56 Hz, NCH_2CH_2), 3.74 (s, 2H, NCH_2Si), 3.62 (m, 2H, OCH_2CH_2), 3.52 (m, 2H, OCH_2CH_2), 3.35 (s, 3H, OCH_3), 0.21 (s, 6H, $Si(CH_3)_2$), 0.08 (s, 9H, $Si(CH_3)_3$). **(^{13}C {^{1}H}, $CDCl_3$)** δ ppm: 135.7 (s, NCHN), 123.4 (s, NCHCHN), 122.6 (s, NCHCHN), 119.9 (q, *J*=321.1 Hz, (CF_3)), 71.6 (s, NCH_2Si), 70.3 (s, NCH_2CH_2O), 68.8 (s, NCH_2CH_2O), 59.0 (s, OCH_2CH_2O), 49.8 (s, OCH_2CH_2O), 42.5 (s, OCH_3), 1.8 (s, $Si(CH_3)_2$), –1.1 (s, $Si(CH_3)_3$). **(^{29}Si {^{1}H}, $CDCl_3$)** δ ppm: 6.55 (s, $Si(CH_3)_2$), 2.93 (s, $Si(CH_3)_3$). **(^{19}F $CDCl_3$)** δ ppm: –78.19 (s, CF_3). **MS m/z (EI):** 332.25, 331.25, 185.05, 154.10, 147.05, 96.00. **IR (**neat**):** 3150.6 w, 2959.3 w, 1562.5 w, 1350.3 m, 1183.3 s, 1052.7 s, 842.7 s.

1-(2-(2-methoxyethoxy)ethyl)-3-(2-methoxyethyl)-1H-imidazol-3-ium bis((trifluoromethyl)-sulfonyl)imide (3): The reaction/workup given for **1** was repeated with **3a** (7.383 g, 20.72 mmol), LiTFSI (6.545 g, 22.79 mmol) and 25 mL of acetone. This gave **3** as light yellow oil (7.290 g, 14.31 mmol, 69%).
NMR: (^{1}H, $CDCl_3$) δ ppm: 8.80 (s, 1H, NC*H*N), 7.46 (t, *J*=1.7 Hz, 1H, NC*H*CHN), 7.38 (t, *J*=1.7 Hz, 1H, NCHC*H*N), 4.37 – 4.34 (m, 4H, $N(CH_2)_2CH_2O$), 3.84 (t, *J*=4.7 Hz, 2H, $NCH_2CH_2OCH_3$), 3.71 (t, *J*=4.7 Hz, 2H, $NCH_2CH_2OCH_2$), 3.66 – 3.63 (m, 2H, OCH_2CH_2O), 3.53 – 3.51 (m, 2H, OCH_2CH_2O), 3.37 (s, 3H, $NCH_2CH_2OCH_3$), 3.36 (s, 3H, $OCH_2CH_2OCH_3$). **(^{13}C {^{1}H}, $CDCl_3$)** δ ppm: 136.34 (s, NCHN), 122.99 (d, *J*=25.6 Hz, NCHCHN), 119.88 (q, *J*=321.6 Hz, CF_3), 71.63 (s), 70.37 (s), 69.98 (s), 68.66 (s), 59.07 (s), 50.03 (d, *J*=21.0 Hz, $O(CH_3)_2$). **(^{19}F $CDCl_3$)** δ ppm: 78.85 (s, CF_3). **MS m/z (EI):** 229.20, 154.10, 140.10, 126.26, 59.56. **IR** (neat**):** 3153.9 w, 2938.2 w, 2883.6 w, 2822.8 w, 1564.9 w, 1453.6 w, 1349.1 m, 1181.4 s, 1133.3 s, 1053.4 s.

1-((1,1,3,3,3-pentamethyldisiloxanyl) methyl) -3-((trimethylsilyl) methyl) -1H-imidazol-3-ium bis ((trifluoromethyl) sulfonyl)amide (4): The reaction/workup given for **1** was repeated with **4a** (9.294 g, 21.00 mmol), LiTFSI (7.234 g, 25.2 mmol), and 30 mL of acetone. This gave **4** as light yellow oil (11.761 gm, 19.74 mmol, 94%).
NMR: (^{1}H, $CDCl_3$) δ ppm: 8.65 (s, 1H, NC*H*N), 7.16 (t, *J*=1.7 Hz, 1H, NC*H*CHCN), 7.10 (t, *J*=1.7 Hz, 1H, NCHC*H*CN), 3.84 (s, 2H,

NCH_2SiO), 3.78 (s, 2H, NCH_2Si), 0.18 (s, 6H, Si(CH_3)$_2$), 0.13 (s, 9H, OSi(CH_3)$_3$), 0.09 (s, 9H, Si(CH_3)$_3$). **(^{13}C {^{1}H, CDCl$_3$}** δ ppm: 134.5 (s, NC*H*N), 123.1 (d, *J*=11.0 Hz, NC*H*CHCN), 119.88 (q, *J* =321.2 Hz, *C*F$_3$), 42.2 (s, NCH_2SiO), 41.8 (s, NCH_2Si), 1.7 (s, Si(CH_3)$_2$), –1.3 (s, OSi(CH_3)$_3$), –3.3 (s, Si(CH_3)$_3$). **(^{29}Si {^{1}H}, CDCl$_3$)** δ ppm**:** 3.61 (s, O*Si*(CH$_3$)$_2$), 3.04 (s, O*Si*(CH$_3$)$_3$), not detected (CH$_2$-*Si*(CH$_3$)$_3$). **(^{19}F CDCl$_3$)** δ ppm: –78.77 (s, CF_3). **MS m/z (EI):** 329.23, 263.12, 229.45, 154.12, 125.56, 99.23, 57.01, 51.23 **IR** (neat): 3146.5 *b*, 2960.9 *w*, 1559.7 *w*, 1350.3 *m*, 1184.7 *s*, 1135.6 *m*, 1052.7 *s*, 841.8 *b*.

1-(2-methoxyethyl)-3-((1,1,3,3,3-pentamethyldisiloxanyl)methyl)-1H-imidazol-3-ium iodide (1a): A mixture of **1b** (4.002 g, 31.69 mmol), **6** (10.963 g, 38.03 mmol) and 30 mL acetonitrile prepared in inert atmosphere was transferred into 100 mL microwave Teflon vials. The reaction mixture was microwave irradiated with controlled temperature programming of 150 °C within 2 min ramp and then held for 40 min at 150 °C, with pressure limit 18 bar, and max power limit of 500 W. The reaction progress was monitored by ^{1}H NMR after collecting the sample from vials. After completion, the reaction mixture was concentrated in *rotavac.* The viscous precipitate was obtained upon drop-wise addition of residue in 50 mL cold ether. The two phase system was kept at 0 °C for 2 h. The ether layer was decanted and the residue was washed with cold ether (50 mL × 3). The yellow viscous liquid was dried in vacuum at 60 °C to give **1a** (8.863 g, 21.39 mmol, 91%).

NMR: (^{1}H, CDCl$_3$) δ ppm: 9.66 (s, 1H, NC*H*N), 7.62 (s, 1H, NC*H*CHN), 7.20 (s, 1H, NCHC*H*N), 4.58 (t, *J*=4.6 Hz, 2H, NCH_2CH$_2$O), 3.89 (s, 2H, NCH_2Si), 3.77 (t, *J*=4.8 Hz, 2H, NCH$_2$CH_2O), 3.34 (s, 3H, OCH_3), 0.21 (s, 6H, Si(CH_3)$_2$), 0.06 (s, 9H, Si(CH_3)$_3$). **(^{13}C {^{1}H}, CDCl$_3$)** δ ppm: 136.1 (s, N*C*HN), 123.2 (s, N*C*HCHN), 122.3 (s, NCH*C*HN), 70.3 (s, NCH$_2$CH$_2$O), 59.1 (s, NCH$_2$Si), 50.0 (s, NCH$_2$*C*H$_2$O), 42.6 (s, O*C*H$_3$), 1.9 (s, Si(*C*H$_3$)$_2$), –0.6 (s, Si(*C*H$_3$)$_3$). **(^{29}Si {^{1}H}, CDCl$_3$)** δ ppm**:** 6.00 (s, *Si*(CH$_3$)$_2$), 3.05 (s, *Si*(CH$_3$)$_3$).

1-(2-(2-methoxyethoxy)ethyl)-3-((1,1,3,3,3-pentamethyldisiloxanyl)methyl)-1H-imidazol-3-ium iodide (2a): The reaction/workup given for **1a** was repeated with **2b** (4.001 g, 23.50 mmol), **6** (8.133 g, 28.21 mmol), and 30 mL of acetonitrile. This gave **2a** (9.150 g, 19.96 mmol, 85% yield) as yellow viscous liquid.

NMR: (^{1}H, CDCl$_3$) δ ppm: 9.50 (s, 1H, NC*H*N), 7.67 (t, *J*=1.7 Hz, 1H, NC*H*CHN), 7.18 (t, *J*=1.7 Hz, 1H, NCHC*H*N), 4.52 (t, *J*=4.6 Hz, 2H, NCH_2CH$_2$O), 3.82 (s, 2H, NCH_2Si), 3.82 (t, *J*=4.3 Hz, 2H, NCH$_2$CH_2O), 3.58 – 3.55 (m, 2H, OCH_2CH$_2$O), 3.43 – 3.41 (m, 2H, OCH$_2$CH_2O), 3.25 (s, 3H, OCH_3), 0.14 (s, 6H, Si(CH_3)$_2$), –0.02 (s, 9H, Si(CH_3)$_3$). **(^{13}C {^{1}H}, CDCl$_3$)** δ ppm: 135.7 (s, N*C*HN), 123.2 (s, N*C*HCHN), 122.2 (s, NCH*C*HN), 71.4 (s, NCH_2Si), 70.1 (s, N*C*H$_2$CH$_2$O), 68.7 (s, NCH$_2$*C*H$_2$O), 58.8 (s, OCH_2CH$_2$O), 49.5 (s, OCH$_2$*C*H$_2$O), 42.4 (s, O*C*H$_3$), 1.7 (s, Si(*C*H$_3$)$_2$), –0.8 (s, Si(*C*H$_3$)$_3$). **(^{29}Si {^{1}H}, CDCl$_3$)** δ ppm: 6.38 (s, *Si*(CH$_3$)$_2$), 2.86 (s, *Si*(CH$_3$)$_3$).

Preparation of 1-(2-(2-methoxyethoxy)ethyl)-3-(2-methoxyethyl)-1H-imidazol-3-ium iodide (3a): The reaction/workup given for **1a** was repeated with **2b** (4.058 g, 23.50 mmol), 2-methoxyethyl 4-methylbenzenesulfonate (**8**, 4.743 g, 25.50 mmol) and 30 mL acetonitrile. This gave **3a** (7.617 g, 21.38 mmol, 91% yield) as yellow viscous liquid.

NMR: (^{1}H, CDCl$_3$) δ ppm: 9.76 (s, 1H, NC*H*N), 7.61 (s, 1H, NC*H*CHN), 7.53 (s, 1H, NCHC*H*N), 4.58 – 4.51 (m, 4H, N(CH_2)$_2$CH$_2$O), 3.97 (m, 2H, NCH$_2$CH_2OCH$_3$), 3.78 (m, 2H, NCH$_2$CH_2OCH$_2$), 3.67 – 3.64 (m, 2H, OCH_2CH$_2$O), 3.53 – 3.49 (m, 2H, OCH$_2$CH_2O), 3.36 (s, 3H, NCH$_2$CH$_2$OCH_3), 3.35 (s, 3H, OCH$_2$CH$_2$OCH_3). **(^{13}C {^{1}H}, CDCl$_3$)** δ ppm: 136.7 (s, N*C*HN), 122.9 (d, *J*=23.7 Hz, NC*H*CHN), 71.6 (s), 70.3 (d, *J*=26.5 Hz), 68.8 (s), 59.1 (d, *J*=11.4 Hz), 50.0 (d, *J*=21.2 Hz).

1-(trimethylsilyl)-3-((1,1,3,3,3-pentamethyldisiloxanyl)methyl)-1H-imidazol-3-ium iodide (4a): The reaction/workup given for **1a** was repeated with **4b** (3.548 g, 23 mmol), **6** (7.963 g, 27.60 mmol) and 30 mL of acetonitrile. This gave **4a** (8.94 g, 20.24 mmol, 88% yield) as yellow viscous liquid.

NMR: (^{1}H, CDCl$_3$) δ ppm: 9.92 (s, 1H, NC*H*N), 7.18 (d, *J*=1.4 Hz, 2H, NC*HCH*CN), 4.03 (s, 2H, NCH_2SiO), 3.96 (s, 2H, NCH_2Si), 0.22 (s, 6H, Si(CH_3)$_2$), 0.17 (s, 9H, OSi(CH_3)$_3$), 0.08 (s, 9H, Si(CH_3)$_3$). **(^{13}C {^{1}H, CDCl$_3$)** δ ppm: 135.1 (s, N*C*HN), 122.8 (s, OSiN*C*HCHNSi), 122.7 (s, OSiNCH*C*HNSi), 42.5 (s, NCH$_2$SiO), 42.0 (s, NCH$_2$Si), 1.9 (s, Si(*C*H$_3$)$_2$), –0.8 (s, OSi(*C*H$_3$)$_3$), –2.7 (s, CH$_2$Si(*CH*$_3$)$_3$). **(^{29}Si {^{1}H}, CDCl$_3$)** δ ppm**:** 3.61 (s, *Si*(CH$_3$)$_2$), 3.04 (s, O*Si*(CH$_3$)$_3$), –135.90 (s, *Si*(CH$_3$)$_3$).

Microwave synthesis of bulk scale [BMIM]$^+$ Br$^–$ (5a): A mixture of 1-Methyl imidazole (164.200 g, 2000.00 mmol, d = 1.03) and *n*-Butyl bromide (411.660 g, 3004.38 mmol) were mixed in 1000 mL RB flask and stirred for 30 min at ambient temperature under N_2 atmosphere. The reaction mixture was transferred equally (~60 mL) into eight microwave Teflon vials of 100 mL capacity containing a stir bar. The reaction mixture was microwave irradiated with controlled temperature programming of 150 °C within 2 min ramp and then held for 10 min at 150 °C, with a pressure limit 18 bar, and max power limit of 900 W. The reaction progress was monitored by ^{1}H NMR and TLC (80/20 dichloromethane/methanol in silica gel). The NMR was taken after 10 min from vial containing immersion temperature probe. The ^{1}H NMR shows clean product along with *n*-BuBr which was used in excess (Figure S6, SI). After completion, excess *n*-Butyl bromide was recovered (60.105 g, 438.66 mmol, 43.8% of 137.62 g excess of *n*BuBr) by decanting from the reaction mixture. The viscous IL residue was evacuated in vacuum (1×10^{-3} mbar) at 50 °C for 2 h and more *n*BuBr of 45.374 g, 331.15 mmol were collected from the trap (total 77.0% of 137.62 g). The residue was washed with ethyl acetate (1×100 mL) to remove any high boiling organic impurity. The obtained brown colour product was dried in vacuum at 60 °C for 5 h to give >98% yield (433.35 g, 1977.68 mol, 98.9%). The pure IL solidifies at ambient temperature.

NMR: (^{1}H, CDCl$_3$) δ ppm: 10.17 (s, 1H, NC*H*N), 7.60 (s, 1H, NC*H*CHCN), 7.23 (s, 1H, NCHC*H*CN), 4.23 (t, *J*=7.4 Hz, 2H), 4.01 (s, 3H), 1.79 (pent, *J*=12.8, 7.6 Hz, 2H), 1.26 (sext, *J*=14.8, 7.4 Hz, 2H), 0.83 (t, *J*=7.4 Hz, 3H).

Acknowledgements

This research is supported by the Department of Atomic Energy (DAE), India (2013/37C/57/BRNS) for financial support and Santosh Chavan thanks to UGC for Fellowship.

Notes and references

1 P. Wasserscheid, and P. Schulz, *Ionic liquids in synthesis, Vol. 7*, 2nd ed., Wiley-VCH, Weinheim, **2008**.
2 a) D. Marquardt, Z. Xie, A. Taubert, R. Thomann, and C. Janiak, *Dalton Trans.* 2011, **40**, 8290-8293; b) V. Khare, Z. Li, A. Mantion, A. A. Ayi, S. Sonkaria, A. Voelkl, A. F. Thunemann, and A. Taubert, *J. Mater. Chem.* 2010, **20**, 1332-1339.
3 K. Thiel, T. Klamroth, P. Strauch, and A. Taubert, *Phys. Chem. Chem. Phys.* 2011, **13**, 13537-13543.
4 a) A. E. Visser, R. P. Swatloski, W. M. Reichert, S. T. Griffin, and R. D. Rogers, *Ind. Eng. Chem. Res.* 2000, **39**, 3596-3604; b) D. Han, and K. H. Row, *Molecules* 2010, **15**, 2405-2426.
5 X. Han, and D. W. Armstrong, *Acc. Chem. Res.* 2007, **40**, 1079-1086.
6 a) A. Berthod, M. J. Ruiz-Ángel, and S. Carda-Broch, *J. Chromatogr. A* 2008, **1184**, 6-18; b) Y. Fukaya, A. Tsukamoto, K. Kuroda, and H. Ohno, *Chem. Commun.* 2011, **47**, 1994-1996.
7 X. Sun, H. Luo, and S. Dai, *Chem. Rev.* 2011, **112**, 2100-2128.
8 a) Y. Shen, W. Li, J. Wu, S. Li, H. Luo, S. Dai, and W. Wu, *Dalton Trans.* 2014, **43**, 10023-10032; b) A. Rout, and K. Binnemans, *Dalton Trans.* 2014, **43**, 1862-1872; c) D. R. Raut, and P. K. Mohapatra, *Sep. Sci. Technol.* 2015, **50**, 380-386.
9 A. Somers, P. Howlett, D. MacFarlane, and M. Forsyth, *Lubricants* 2013, **1**, 3-21.
10 F. Zhou, Y. Liang, and W. Liu, *Chem. Soc. Rev.* 2009, **38**, 2590-2599.
11 . Qu, D. G. Bansal, B. Yu, J. Y. Howe, H. Luo, S. Dai, H. Li, P. J. Blau, B. G. Bunting, G. Mordukhovich, and D. J. Smolenski, *ACS Appl. Mater. Interfaces* 2012, **4**, 997-1002.
12 a) A. Fernicola, B. Scrosati, and H. Ohno, *Ionics* 2006, **12**, 95-102; b) M. Galiński, A. Lewandowski, and I. Stępniak, *Electrochim. Acta* 2006, **51**, 5567-5580; c) M. Gorlov, and L. Kloo, *Dalton Trans.* 2008, 2655-2666. d) A. Lahiri, T. J. S. Schubert, B. Iliev and F. Endres, *Phys. Chem. Chem. Phys.*, 2015, DOI**:** 10.1039/C5CP01337B.
13 W. R. Pitner, P. Kirsch, K. Kawata, and H. Shinohara, in *Green Solvents, Vol. 6*, Wiley/VCH, Weinheim, **2010**, pp. 191-201.
14 *Green Solvents, Ionic Liquids,* (Vol. Eds. P. Wasserscheid, A. Stark) in *Handbook of Green Chemistry,* (Eds. P. T. Anastas) *Vol. 6*, Wiley-VCH, **2013**.
15 M. J. Earle, and K. R. Seddon, *Pure Appl. Chem.* **2000**, *72*, 1391-1399.
16 M. Armand, F. Endres, D. R. MacFarlane, H. Ohno, and B. Scrosati, *Nat Mater* 2009, **8**, 621-629.
17 S. S. Mondal, H. Müller, M. Junginger, A. Kelling, U. Schilde, V. Strehmel, and H. J. Holdt, *Chem. Eur. J.* 2014, **20**, 8170-8181.
18 a) Z. B. Zhou, H. Matsumoto, and K. Tatsumi, *ChemPhysChem* 2005, **6**, 1324-1332; b) S. V. Dzyuba, and R. A. Bartsch, *ChemPhysChem* 2002, **3**, 161-166.
19 D. R. MacFarlane, J. Golding, S. Forsyth, M. Forsyth, and G. B. Deacon, *Chem. Commun.* 2001, 1430-1431.
20 Z.-B. Zhou, H. Matsumoto, and K. Tatsumi, *Chem. Eur. J.* 2005, **11**, 752-766.
21 Z. Chen, S. Liu, Z. Li, Q. Zhang, and Y. Deng, *New J. Chem.* 2011, **35**, 1596-1606.
22 a) L. J. A. Siqueira, and M. C. C. Ribeiro, *J. Phys. Chem. B* 2009, **113**, 1074-1079; b) A. Triolo, O. Russina, R. Caminiti, H. Shirota, H. Y. Lee, C. S. Santos, N. S. Murthy, and E. W. Castner, Jr., *Chem. Commun.* 2012, **48**, 4959-4961.
23 Y. Jin, S. Fang, M. Chai, L. Yang, and S.-i. Hirano, *Ind. Eng. Chem. Res.* 2012, **51**, 11011-11020.
24 H. Shirota, J. F. Wishart, and E. W. Castner, *J. Phys. Chem. B* 2007, **111**, 4819-4829.
25 Z. J. Chen, T. Xue, and J.-M. Lee, *RSC Adv.* 2012, **2**, 10564-10574.
26 A. K. Burrell, R. E. D. Sesto, S. N. Baker, T. M. McCleskey, and G. A. Baker, *Green Chem.* 2007, **9**, 449-454.
27 a) C. O. Kappe, A. Stadler, D. Dallinger, *Microwaves in organic and medicinal chemistry*, John Wiley & Sons, **2012**; b) M. Deetlefs, and K. R. Seddon, *Green Chem.* 2010, **12**, 17-30; c) V. V. Namboodiri, and R. S. Varma, *Tetrahedron Lett.* 2002, **43**, 5381-5383; d) R. S. Varma, and V. V. Namboodiri, *Chem. Commun.* 2001, 643-644; e) M. Deetlefs, and K. R. Seddon, *Green Chem.* 2003, ***5***, 181-186.
28 P. Bonhôte, A.-P. Dias, N. Papageorgiou, K. Kalyanasundaram, and M. Grätzel, *Inorg. Chem.* 1996, **35**, 1168-1178.
29 C. A. Angell, *Chem. Rev.* 2002, **102**, 2627-2650.
30 Z. Fei, W. H. Ang, D. Zhao, R. Scopelliti, E. E. Zvereva, S. A. Katsyuba, and P. J. Dyson, *J. Phys. Chem. B* 2007, **111**, 10095-10108.
31 S. Bulut, M. A. Ab Rani, T. Welton, P. D. Lickiss, and I. Krossing, *ChemPhysChem* 2012, **13**, 1802-1805.
32 C. P. Fredlake, J. M. Crosthwaite, D. G. Hert, S. N. V. K. Aki, and J. F. Brennecke, *J. Chem. Eng. Data* 2004, **49**, 954-964.
33 J. G. Huddleston, A. E. Visser, W. M. Reichert, H. D. Willauer, G. A. Broker, and R. D. Rogers, *Green Chem.* 2001, **3**, 156-164.
34 D. M. Fox, W. H. Awad, J. W. Gilman, P. H. Maupin, H. C. De Long, and P. C. Trulove, *Green Chem.* 2003, **5**, 724-727.
35 N. Calvar, E. Gómez, E. A. Macedo, and Á. Domínguez, *Thermochim. Acta* 2013, **565**, 178-182.

[1] P. Wasserscheid, P. Schulz, *Ionic liquids in synthesis, Vol. 7*, 2nd ed., Wiley-VCH, Weinheim, **2008**.
[2] aD. Marquardt, Z. Xie, A. Taubert, R. Thomann, C. Janiak, *Dalton Trans.* **2011**, *40*, 8290-8293; bV. Khare, Z. Li, A. Mantion, A. A. Ayi, S. Sonkaria, A. Voelkl, A. F. Thunemann, A. Taubert, *J. Mater. Chem.* **2010**, *20*, 1332-1339.
[3] K. Thiel, T. Klamroth, P. Strauch, A. Taubert, *Phys. Chem. Chem. Phys.* **2011**, *13*, 13537-13543.
[4] aA. E. Visser, R. P. Swatloski, W. M. Reichert, S. T. Griffin, R. D. Rogers, *Ind. Eng. Chem. Res.* **2000**, *39*, 3596-3604; bD. Han, K. H. Row, *Molecules* **2010**, *15*, 2405-2426.
[5] X. Han, D. W. Armstrong, *Acc. Chem. Res.* **2007**, *40*, 1079-1086.
[6] aA. Berthod, M. J. Ruiz-Ángel, S. Carda-Broch, *J. Chromatogr. A* **2008**, *1184*, 6-18; bY. Fukaya, A. Tsukamoto, K. Kuroda, H. Ohno, *Chem. Commun.* **2011**, *47*, 1994-1996.
[7] X. Sun, H. Luo, S. Dai, *Chem. Rev.* **2011**, *112*, 2100-2128.
[8] aY. Shen, W. Li, J. Wu, S. Li, H. Luo, S. Dai, W. Wu, *Dalton Trans.* **2014**, *43*, 10023-10032; bA. Rout, K. Binnemans, *Dalton Trans.* **2014**, *43*, 1862-1872; cD. R. Raut, P. K. Mohapatra, *Sep. Sci. Technol.* **2015**, *50*, 380-386.
[9] A. Somers, P. Howlett, D. MacFarlane, M. Forsyth, *Lubricants* **2013**, *1*, 3-21.
[10] F. Zhou, Y. Liang, W. Liu, *Chem. Soc. Rev.* **2009**, *38*, 2590-2599.

[11] J. Qu, D. G. Bansal, B. Yu, J. Y. Howe, H. Luo, S. Dai, H. Li, P. J. Blau, B. G. Bunting, G. Mordukhovich, D. J. Smolenski, *ACS Appl. Mater. Interfaces* **2012**, *4*, 997-1002.
[12] aA. Fernicola, B. Scrosati, H. Ohno, *Ionics* **2006**, *12*, 95-102; bM. Galiński, A. Lewandowski, I. Stępniak, *Electrochim. Acta* **2006**, *51*, 5567-5580; cM. Gorlov, L. Kloo, *Dalton Trans.* **2008**, 2655-2666.
[13] W. R. Pitner, P. Kirsch, K. Kawata, H. Shinohara, in *Green Solvents, Vol. 6*, Wiley/VCH, Weinheim, **2010**, pp. 191-201.
[14] *Handbook of Green Chemistry, Vol. 6*, Wiley-VCH, **2013**.
[15] M. J. Earle, K. R. Seddon, *Pure Appl. Chem.* **2000**, *72*, 1391-1399.
[16] M. Armand, F. Endres, D. R. MacFarlane, H. Ohno, B. Scrosati, *Nat Mater* **2009**, *8*, 621-629.
[17] S. S. Mondal, H. Müller, M. Junginger, A. Kelling, U. Schilde, V. Strehmel, H. J. Holdt, *Chem. Eur. J.* **2014**, *20*, 8170-8181.
[18] aZ. B. Zhou, H. Matsumoto, K. Tatsumi, *ChemPhysChem* **2005**, *6*, 1324-1332; bS. V. Dzyuba, R. A. Bartsch, *ChemPhysChem* **2002**, *3*, 161-166.
[19] D. R. MacFarlane, J. Golding, S. Forsyth, M. Forsyth, G. B. Deacon, *Chem. Commun.* **2001**, 1430-1431.
[20] Z.-B. Zhou, H. Matsumoto, K. Tatsumi, *Chem. Eur. J.* **2005**, *11*, 752-766.
[21] Z. Chen, S. Liu, Z. Li, Q. Zhang, Y. Deng, *New J. Chem.* **2011**, *35*, 1596-1606.
[22] aL. J. A. Siqueira, M. C. C. Ribeiro, *J. Phys. Chem. B* **2009**, *113*, 1074-1079; bA. Triolo, O. Russina, R. Caminiti, H. Shirota, H. Y. Lee, C. S. Santos, N. S. Murthy, E. W. Castner, Jr., *Chem. Commun.* **2012**, *48*, 4959-4961.
[23] Y. Jin, S. Fang, M. Chai, L. Yang, S.-i. Hirano, *Ind. Eng. Chem. Res.* **2012**, *51*, 11011-11020.
[24] H. Shirota, J. F. Wishart, E. W. Castner, *J. Phys. Chem. B* **2007**, *111*, 4819-4829.
[25] Z. J. Chen, T. Xue, J.-M. Lee, *RSC Adv.* **2012**, *2*, 10564.
[26] A. K. Burrell, R. E. D. Sesto, S. N. Baker, T. M. McCleskey, G. A. Baker, *Green Chem.* **2007**, *9*, 449-454.
[27] aC. O. Kappe, A. Stadler, D. Dallinger, *Microwaves in organic and medicinal chemistry*, John Wiley & Sons, **2012**; bM. Deetlefs, K. R. Seddon, *Green Chem.* **2010**, *12*, 17-30; cV. V. Namboodiri, R. S. Varma, *Tetrahedron Lett.* **2002**, *43*, 5381-5383; dR. S. Varma, V. V. Namboodiri, *Chem. Commun.* **2001**, 643-644; eM. Deetlefs, K. R. Seddon, *Green Chem.* **2003**, *5*, 181-186.
[28] P. Bonhôte, A.-P. Dias, N. Papageorgiou, K. Kalyanasundaram, M. Grätzel, *Inorg. Chem.* **1996**, *35*, 1168-1178.
[29] C. A. Angell, *Chem. Rev.* **2002**, *102*, 2627-2650.
[30] Z. Fei, W. H. Ang, D. Zhao, R. Scopelliti, E. E. Zvereva, S. A. Katsyuba, P. J. Dyson, *J. Phys. Chem. B* **2007**, *111*, 10095-10108.
[31] S. Bulut, M. A. Ab Rani, T. Welton, P. D. Lickiss, I. Krossing, *ChemPhysChem* **2012**, *13*, 1802-1805.
[32] C. P. Fredlake, J. M. Crosthwaite, D. G. Hert, S. N. V. K. Aki, J. F. Brennecke, *J. Chem. Eng. Data* **2004**, *49*, 954-964.
[33] J. G. Huddleston, A. E. Visser, W. M. Reichert, H. D. Willauer, G. A. Broker, R. D. Rogers, *Green Chem.* **2001**, *3*, 156-164.
[34] D. M. Fox, W. H. Awad, J. W. Gilman, P. H. Maupin, H. C. De Long, P. C. Trulove, *Green Chem.* **2003**, *5*, 724-727.
[35] Y. Cao, T. Mu, *Ind. Eng. Chem. Res.* **2014**, *53*, 8651-8664.
[36] N. Calvar, E. Gómez, E. A. Macedo, Á. Domínguez, *Thermochim. Acta* **2013**, *565*, 178-182.